



NLR TP 97630

## **Overview of the NH90 wind tunnel test activities and the benefits to the helicopter development**

C. Hermans, J. Hakkaart, G. Panosetti, G. Preatoni,  
V. Mikulla, F. Chéry, C. Serr

## DOCUMENT CONTROL SHEET

	<b>ORIGINATOR'S REF.</b> TP 97630 U		<b>SECURITY CLASS.</b> Unclassified																					
<b>ORIGINATOR</b> National Aerospace Laboratory NLR, Amsterdam, The Netherlands																								
<b>TITLE</b> Overview of the NH90 wind tunnel test activities and the benefits to the helicopter development																								
<b>PRESENTED AT</b> the American Helicopter Society 53rd Annual Forum, Virginia Beach, Virginia (U.S.A.), April 29-May 1, 1997																								
<b>AUTHORS</b> C. Hermans, J. Hakkaart, G. Panosetti, G. Preatoni, V. Mikulla, F. Chéry, C. Serr		<b>DATE</b> 971211	<b>pp ref</b> 22																					
<b>DESCRIPTORS</b> <table style="width: 100%; border: none;"> <tr> <td style="width: 33%;">Aerodynamic drag</td> <td style="width: 33%;">Helicopter design</td> <td style="width: 33%;">Powered models</td> </tr> <tr> <td>Aerodynamics</td> <td>Helicopter tail rotors</td> <td>Scale models</td> </tr> <tr> <td>Air intakes</td> <td>Infrared signatures</td> <td>Wind tunnel tests</td> </tr> <tr> <td>Engine inlets</td> <td>Lifting rotors</td> <td></td> </tr> <tr> <td>Exhaust gases</td> <td>Measuring instruments</td> <td></td> </tr> <tr> <td>Flight characteristics</td> <td>Military helicopters</td> <td></td> </tr> <tr> <td>Flight mechanics</td> <td>Models</td> <td></td> </tr> </table>				Aerodynamic drag	Helicopter design	Powered models	Aerodynamics	Helicopter tail rotors	Scale models	Air intakes	Infrared signatures	Wind tunnel tests	Engine inlets	Lifting rotors		Exhaust gases	Measuring instruments		Flight characteristics	Military helicopters		Flight mechanics	Models	
Aerodynamic drag	Helicopter design	Powered models																						
Aerodynamics	Helicopter tail rotors	Scale models																						
Air intakes	Infrared signatures	Wind tunnel tests																						
Engine inlets	Lifting rotors																							
Exhaust gases	Measuring instruments																							
Flight characteristics	Military helicopters																							
Flight mechanics	Models																							
<b>ABSTRACT</b> <p>In the framework of the Design &amp; Development (D&amp;D) phase of the NH90 helicopter program, a wind tunnel test program is carried out using various sub-scale models to determine the aerodynamic behaviour of the vehicle.</p> <p>Approximately 1900 hours of wind tunnel tests have been conducted since 1987 in the Netherlands (Low Speed wind Tunnel LST and German Dutch Wind tunnel DNW) and in France (Eurocopter France ECF low speed wind tunnel). The National Aerospace Laboratory NLR conducted tests with a drag model and powered models (partial tail rotor model and main rotor model, including engine installation modules). At ECF partial models of the air intake system and exhaust system have been tested extensively. Rotor/interaction models were used for stabilizer trade studies. Engine intake and exhaust configuration studies were conducted. Rotor performance and helicopter stability were verified. A series of fuselage model tests were conducted to assist in airframe development. The availability of a range of dedicated (powered) models and execution of wind tunnel tests was a substantial contribution to the development risk reduction effort performed for the multinational NH90 helicopter program.</p>																								

# OVERVIEW OF THE NH90 WIND TUNNEL TEST ACTIVITIES AND THE BENEFITS TO THE HELICOPTER DEVELOPMENT

by

Christophe Hermans, Joost Hakkaart (National Aerospace Laboratory NLR)  
Giuseppina Panosetti, Gaetano Preatoni (Agusta SpA)  
Volker Mikulla (Eurocopter Deutschland)  
François Chéry, Christophe Serr (Eurocopter France)

## Abstract

In the framework of the Design & Development (D&D) phase of the NH90 helicopter program, a wind tunnel test program is carried out using various sub-scale models to determine the aerodynamic behaviour of the vehicle.

Approximately 1900 hours of wind tunnel tests have been conducted since 1987 in the Netherlands (Low Speed wind Tunnel LST and German Dutch Wind tunnel DNW) and in France (Eurocopter France ECF low speed wind tunnel). The National Aerospace Laboratory NLR conducted tests with a drag model and powered models (partial tail rotor model and main rotor model, including engine installation modules). At ECF partial models of the air intake system and exhaust system have been tested extensively.

Rotor/interaction models were used for stabilizer trade studies. Engine intake and exhaust configuration studies were conducted. Rotor performance and helicopter stability were verified. A series of fuselage model tests were conducted to assist in airframe development.

The availability of a range of dedicated (powered) models and execution of wind tunnel tests was a substantial contribution to the development risk reduction effort performed for the multinational NH90 helicopter program.

## Notation

ADS	Air Data System
AIP	Aerodynamic Interface Plane
D&D	Design & Development
DLR	Deutsche Versuchsanstalt für Luft und Raumfahrt
DNW	Duits Nederlandse Windtunnel (German Dutch Wind tunnel)
ECD	Eurocopter Deutschland
ECF	Eurocopter France
FPDS	Feasibility Pre-Definition Study

IRS	Infra Red System
LH	Left Hand
LST	Low Speed wind Tunnel
MWM	Modular Wind tunnel Model
NAHEMA	NATO Helicopter Management Agency
NFH	NATO Frigate Helicopter
NH90	NATO Helicopter for the 90-ties
NIAG	NATO Industrial Advisory Group
NLR	Nationaal Lucht- en Ruimtevaart Laboratorium
PCB	Printed Circuit Board
PDP	Project Definition Phase
RH	Right Hand
TTH	Tactical Transport Helicopter

## NH90, helicopter of the third millennium

Studies conducted by NATO Industrial Advisory Group "NIAG SG14" in the early eighties are the conceptual origin of the NH90 program. The Memorandum of Understanding for the full development was signed in December 1990 by the four nations: France, Italy, Germany and The Netherlands.

In February 1992, the four participating Governments constituted an international program office, called NAHEMA (NATO Helicopter Management Agency). The four companies sharing the Design and Development of the NH90 Program (Agusta, Eurocopter Deutschland, Eurocopter France and Fokker Aerostructures) signed an Intercompany Agreement in March 1992 and established a joint venture, the company NHIndustries, to ensure international industrial program management. The Dutch industrial participation is shared between Fokker Aerostructures, SP Aerospace and Vehicle Systems (former DAF SP) and the National Aerospace Laboratory NLR.

The NH90 is a unique integrated weapon system developed in two mission variants from a common basic model (figure 1).

The Tactical Transport Helicopter (TTH) is the transport version, primarily for tactical transport of personnel (14-20 troops) and material (more than



*Fig.1: NH90 prototype 1 (PT1) in flight*

2500 kg of cargo), heliborne operations and Search And Rescue. This version is optimised for low signatures (acoustic, radar, infrared) and it will be equipped with a night vision system (Tactical Forward Looking Infra Red, Night Vision Goggles, Helmet Mounted Sight & Display), Obstacle Warning System, defensive weapons suite, passive and active measures against the threat. The TTH is designed for high manoeuvrability in Nap of the Earth operations. Because of its features, characteristics and systems integration, it is capable of operating successfully by day and night/adverse weather conditions in any environment.

The NATO Frigate Helicopter (NFH) is the naval version, primarily for autonomous Anti-Submarine Warfare, Anti Surface Unit Warfare missions. The helicopter is designed for day & night/adverse weather /severe ship motion environment operations. Equipped with a basic and mission avionics system, the NFH version will be capable of performing the mission autonomously with a crew of three. Its capabilities include launch and recovery from small vessels in extreme adverse weather conditions.

The NH90 is a twin engine helicopter in the 9 ton class. Some outstanding examples of innovative technologies are the extended use of composite materials, the high level of system integration and modularity, the aerodynamic design, the low detectability, the optimised man-machine interface minimising the pilot and crew workload, the high level of safety (with adequate "one engine inoperative" performance) and the overall crashworthiness characteristics.

At the start of D&D, the estimated need of the four Navies (France, Italy, Germany, and The Netherlands), of the three Armies (France, Italy, Germany) and the German Air Force was 726 aircrafts; 544 in the Tactical

Transport version (TTH) and 182 in the Naval version (NFH). The industrial share during the Design and Development phase is configured in proportion to their national need (ECF 42.4 %, Agusta 26.9 %, ECD 24.0 % and Fokker 6.7 %).

The NH90 helicopter (first of five prototypes) made its public debut on February 15, 1996 at Eurocopter France's facility in Marignane (France). Prototype 1, shown in figure 2, successfully accumulated 75 flying hours in 1996.



*Fig.2: First flight of PT1 at ECF, Marignane*

This first prototype represents the basic airframe design, based on thorough tests (both laboratory and wind tunnel) and evaluations to reduce development risks.

### **Scope of wind tunnel test program**

First wind tunnel testing was already performed prior to the start of the Design & Development phase (figure 3). During the Feasibility Pre-Definition Study (FPDS) a low speed wind tunnel investigation was carried out at a scale 1:10 drag model to discover possible problem areas at the earliest possible stage of the program and to compile a database supporting discussions concerning fuselage shape.

In the Project Definition Phase (PDP) a second series of tests was performed to determine the aerodynamic characteristics of the NH90 helicopter, which shape had evolved since. Furthermore the model suspension in the DNW-LST was improved, by applying a strut support system, with only one pitching moment wire for angle of attack adjustment.

To minimize the technical development risk and demonstrate the feasibility of stringent technical

objectives in an early stage of the development, a wind tunnel program was included in the scope of work for the Design and Development phase.

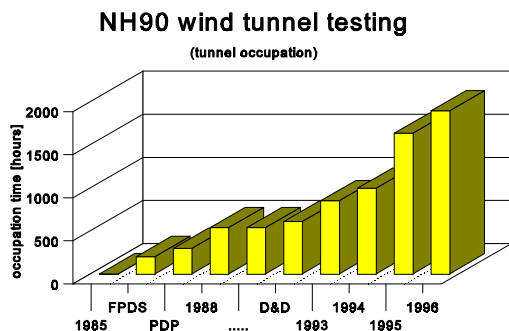


Fig.3 Accumulated wind tunnel testing time

At the beginning of the D&D a comprehensive list of wind tunnel test needs was compiled and priorities were assigned. Various wind tunnel model configurations were defined that could fulfil the major part of the high priority test needs in the most efficient way within the program constraints, like schedule and budget.

In summary this lead to the following model definitions:

- a 1:10 scale fuselage (drag) model for testing in the DNW-LST;
- a 1:3.881 scale tail model fitted with a powered tail rotor (DNW-LST);
- a 1:3.881 scale fuselage module fitted to a powered main rotor to be tested in the German Dutch Wind Tunnel (DNW);
- a 1:10 scale engine recirculation model fitted with a 2-bladed powered main rotor and engine/IRS flow simulation in the ECF wind tunnel;
- a 1:3 scale air intake model (ECF wind tunnel).

During the course of the D&D at regular intervals meetings were held with representatives of all partner companies. Test needs identified were assessed and specific wind tunnel test campaigns being initiated. Test needs were transformed into detailed wind tunnel model definitions and a test plan, which contained a global description of the wind tunnel test campaign to be performed (model and sensor definition, data acquisition and processing, data presentation and test matrix). Having finalized the test plan and model definition, activities were being initiated to prepare the test campaign, which included model design and manufacture of new components or existing hardware adaptations.

Fuselage model testing in the DNW-LST comprises approximately 50% of the test effort, accumulated during nine campaigns. The tests focused mainly on the external aerodynamic characteristics of the NH90 helicopter. One campaign was dedicated to the rear ramp; influence of rear ramp position (open, intermediate or closed) on global aerodynamic loads for handling qualities and performance evaluations and on rear ramp and hatch loads for design load verification were assessed.

Powered tail rotor model tests were performed in the DNW-LST to assess the tail rotor efficiency at extreme sidewind conditions and tail rotor - vertical tail interference effects.

The first test campaign in DNW with the powered main rotor model primarily was devoted to the low speed flight characteristics. An extensive database with test results of various horizontal tail configurations was established, supporting the design of the horizontal tail and flight control system. The second test, performed in December 1996, focused on high speed flight conditions and engine air intake pressure losses, exhaust gas recirculation and airframe heating.

One engine recirculation test campaign was conducted in the ECF wind tunnel early 1995 to explore susceptibility to recirculation of various exhaust configurations. Those tests were also useful to measure the impact of different exhausts, including Infra Red System, on the airframe heating. In December 1995 and September 1996, during two entries of the air intake model in the ECF wind tunnel, engine inflow characteristics and installation losses were investigated. Air intake definition was optimised to comply with the helicopter/engine interface criteria.

### Description of wind tunnel models

The following sections contain an overview of the various test objectives and wind tunnel models applied, which characteristics have been summarized in table 1.

#### Fuselage model (scale 1:10)

##### Test objectives

The main objectives to be fulfilled by the fuselage model, are:

- determination of drag and stability characteristics of helicopter configurations;
- assessment of an extensive aerodynamic database for handling quality simulation modelling purposes;
- assessment of the hub and upper deck wake behaviour;
- measurement of the surface pressure

distribution to support the air data sensor positioning and numerical model verification;

- determination of the influence of the rear ramp opening on the handling qualities and performance.

#### Model description

The fuselage (drag) model is a representation on scale 1:10 of the external contour of the NH90 helicopter for testing in the DNW-LST (figure 4). The model comprises of the fuselage, rotating main rotor hub and blade stubs, tail surfaces and other protuberances. The model, designed and manufactured at NLR, has a highly modular structure facilitating exchange of components and investigation of contour modifications. The aerodynamic loads acting on the model are measured with an internal six component strain gauge balance. The model is furthermore equipped with a large number of pressure holes.

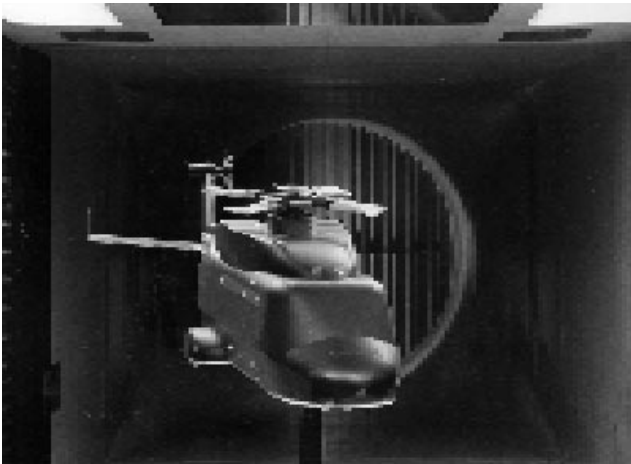


*Fig.4: Fuselage model (1:10) in LST (photo: NLR)*

The model is attached on a sting which on its turn is mounted on the -mechanism ( $\pm 20^\circ$ ) below the floor of the test section. The sideslip angle can be adjusted by rotating the turntable with sting support system about its vertical axis ( $\pm 180^\circ$ ).

The major part of the tests are performed at a tunnel speed of 40 or 75 [m/sec].

The main structural element of the model is a box-like structure, which contains an internal six component strain gauge balance connected to a sting support. The external contour of the model is generated by dividing this shape into a number of modules, that can be mounted on the box. The model can be rolled in the test section over

angles of 0, 90, 180 and 270 by cyclic shifting of the modules around the longitudinal axis of the box.

The main rotor hub, equipped with rounded blade stubs, has the capability to rotate upto 1200 rpm. The blade stub angles, both collective and cyclic, are settable.

Modifications of a module during development testing can be done in a variety of ways, ranging from hand-modelling with plasticine to contour milling of a complete new module. The construction and the choice of the material (aluminum alloy) is such, that the initial configuration can be reproduced accurately after several years of wind tunnel testing.



*Fig.5: Components of fuselage model (photo: NLR)*

The external contour consists of a large number of modules (see figure 5) such as fuselage nose, center part of the fuselage (divided into 4 sections, being the top, bottom and two side walls) and engine cowlings (with intakes and exhausts). The fairing of the main rotor axis (main rotor pylon), main rotor hub (rotating), rear fuselage, tail boom, sponsons (inclusive the cavities for the undercarriage), undercarriage (consisting of the main wheels and the nose wheels), horizontal tail surface (with variable setting angle), vertical tail surface, tail rotor hub (not rotating) and various external stores are also represented as separate items.

The ramp consists of two components (ramp and hatch) which can be opened at various angles.

#### Instrumentation

The aerodynamic loads acting on the model are measured with an internal six component strain gauge balance. Both

1.5" and 2" TASK balances can be mounted inside the model. Dedicated balance calibrations have been performed to adjust the balance calibration range to the expected model loads.

The internal balance measures the global forces on the model only. The aerodynamic loads on the sting itself are not measured. However, the sting disturbs the flow around the model by its displacement flow and the direct effect of the sting on the boundary-layer flow over the bottom of the fuselage model.

This support interference has been obtained from the difference of two measurements. The first run is done with the model inverted (upside-down) and the sting through the roof of the model. The second run is done with the same configuration, but with an additional dummy sting through the bottom of the fuselage (see sketch of figure 6).

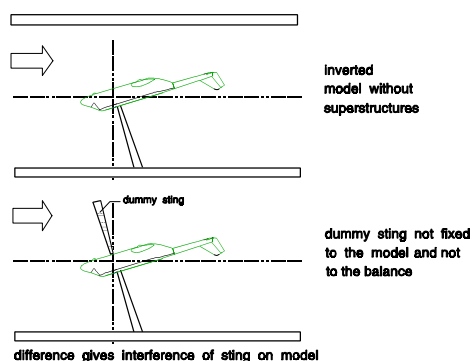


Fig.6: Sting interference measurement approach

The dummy sting is not attached to the model, but to the main sting support (it is a kind of extension of the main sting). The dummy sting has the same external shape as the main sting.

The model is equipped with 125 static pressure holes especially in the nose, aft fuselage and rear ramp area. Surface pressures can be measured with conventional transducers or with an electronic scanning system. The most salient features of this electronic scanning system are the one transducer per orifice concept and the capability to perform in situ calibrations.

To measure the angle of attack accurately, a Q-flex is mounted inside the model

The number of revolutions of the main rotor hub is measured on the shaft of the hub with a slotted opto-switch in combination with a copper disk with six equidistant holes.

Pressure loss and frequency content of the model upper deck and rotor hub wake can be measured with a rake. This wake rake is equipped with 59 total pressure and two unsteady pressure probes at a pitch of 10 [mm]. To be able to traverse the wake rake continuously, optimizing testing time, the data is acquired with an electronic scanning system. The signals of the two unsteady probes are analyzed with a Fourier system to determine the occurring frequencies.

### Powered tail rotor model (scale 1:3.881)

#### Test objectives

The main objectives that are to be fulfilled by the model, are:

- determination of the tail rotor effectiveness at large side wind conditions;
- investigation of the aerodynamic and stability characteristics of the empennage in the presence of the tail rotor wake;
- supporting of performance predictions of the tail rotor-fuselage combination at high flight speeds.

#### Model description

The powered tail rotor model is a partial model (scale 1:3.881) of the NH90, consisting of a powered tail rotor module (hub and blades), vertical tail and the aft part of the tail boom (from tail folding line onwards). The part in front of the tail boom folding hinge is contoured such, that a sound air flow is realized over the empennage part. The vertical fin consists of 4 model parts, i.e. the basic vertical fin configuration, two extensions (on top and at trailing edge) and a tail gearbox fairing. The model allows for limited "isolated" tail rotor testing, since aerodynamic interference of the internal wiring and tubes is large. At the aft part of the tail boom a horizontal tail can be mounted. All model parts that are asymmetrical with respect to the vertical plane of the aircraft are mirrored to that reference plane (see powered main rotor model description for further explanation).

The empennage and tail rotor modules are connected to a support structure, which is mounted to the external tunnel balance the DNW-LST. The sideslip angle of the model can be changed by rotating the complete system (range of 315 ). Figure 7 shows the model set-up in the DNW-LST.

Model design and manufacturing (partially) was subcontracted to Dynamic Engineering Incorporated (DEI). The model was designed to meet specific model tail rotor thrust, power and rpm requirements (worst

case derived from the helicopter tail rotor load spectrum) and vertical tail aerodynamic loads. Although this artificial load case will never occur during wind tunnel testing, it was used to verify model structural integrity. Present model capabilities however are limited by some internal rotor drive system (off-the-shelf) components.



Fig.7: Powered tail rotor model in LST (photo: NLR)

The primary objective of the wind tunnel tests was to investigate the efficiency of the tail rotor/fin assembly, particularly at low speed. Therefore the rotor should be considered as a thrust generator and consequently the (fully articulated) hub design was simplified. The model hub is a flat plate to which the four blades are connected through pins and bearings. The hub is mounted to the end of the rotor drive shaft. The composite tail rotor blades are scaled geometrically (linear twist distribution, OA313 and OARA9M airfoil types). Rotor blades are attached to the hub through a rotor cuff. Geometrical scaling of the blade geometry and flapping hinge location ensures generation of a full scale representative rotor downwash, which is important for the assessment of tail rotor fin interaction characteristics. Blade flapping stops are included in the rotor hub design, precluding fin contact by the blades.

During the design a trade-off has been made between drive system power/speed requirements and model contour envelope, since no drive motors and flex couplings were available that could provide the power and torque required which fit within the contour of the tail.

It was decided to preserve the model contour at the expense of power and speed. The drive motor chosen for the rotor system is a hydraulic motor integrated in the aft tail boom (rated at 13 kW @ 3000 rpm, being approx. 40% of Mach scaling). Drive motor output torque is transmitted through a drive shaft to the tail rotor transmission (gearbox input shaft)

Rotor thrust can be varied by means of remotely controlled blade collective pitch angle control device (range:  $\pm 25^\circ$ ).

#### Instrumentation

Tail rotor thrust and torque are measured with an internal load balance, mounted on the tail rotor gearbox. It uses the reaction principle for all forces including rotating moments. Measurement accuracy is 0.5% of its full load range.

Blade pitch and flapping angle sensors (on two opposite blades) are non-contact devices, using a magnet and a Hall effect transistor. Measurement accuracy is approximately 0.15°. Sensor read-out (rotational system) is fed to a small size slipring. Blade pitch angle back-up measurement redundancy is provided by a LVDT, which measures pitch actuator displacement.

For hydraulic motor rpm control, drive shaft rotational speed is determined by an electro magnetic pick-up, which also features blade azimuth marking.

#### **Powered main rotor model (scale 1:3.881)**

##### Test objectives

The primary test objectives of the scale 1:3.881 powered model are:

- determination of the helicopter trim attitude at low speed and high speed stability characteristics;
- investigation of the fuselage aerodynamic and stability characteristics in the presence of the rotor wake;
- assessment of the engine air intake pressure loss, distortion and gyration;
- determination of exhaust gas recirculation at low speed lateral and rearward flight;
- investigation of airframe heating and exhaust IR signature.

##### Model description

The first test program carried out in DNW concerned an experiment on a fuselage model of the NH90 helicopter, equipped with a powered main rotor, driven by the DLR (Deutsche Forschungsanstalt für Luft- und Raumfahrt) Modular Wind tunnel Model MWM rotor test rig.



The model scale (1:3.881) was dictated by the fact that use was made of an existing model main rotor system (i.e. rotor hub and blades owned by Eurocopter). The blades of this rotor resembled the NH90 blades as to planform and sectional profiles, but the weight was about double. The hub as a consequence was much more massive and voluminous than a properly geometrically scaled down NH90 hub. In view of the goals for the first test, these deficiencies however were considered to be of only minor importance, since the emphasis was put on realizing a proper simulation of the downwash field of the main rotor.

The model fuselage was manufactured from glass fibre reinforced resin in order to obtain a light weight, but stiff structure.

Because of the reversed sense of rotation of the existing model main rotor system, as compared to the actual NH90 main rotor, the aft part of the tail boom and the vertical fin are manufactured as mirrored images with respect to the actual fuselage. For the same reason the tail rotor gearbox fairing, the tail rotor hub and the horizontal stabilizer were mirror imaged with respect to the fuselage longitudinal plane. The fuselage can be equipped with a variety of horizontal stabilizers, varying in configuration (e.g. slat), size and/or location.

The rotor system is driven through the rotor test rig MWM. This system is operated by a crew of the Flight Mechanics Department of DLR. MWM drives the rotor system with a hydraulic motor. Furthermore it controls the settings of the rotor blades and measures the loads generated by the rotating rotor by means of a built-in balance system, composed of six strain gauged load transducers. Both the number of revolutions of the rotor and the swashplate settings are remotely controllable in order to achieve a nominal model load condition.

For the second test entry in DNW, a dedicated NH90 powered main rotor model has been developed by NLR, to properly represent the rotor system high speed behaviour. The fully articulated 4 bladed main rotor system consists of a hub connected to a drive shaft. Rotor radius is 2.10 [m]. To ensure representative rotor system wakes and related drag characteristics of the full scale NH90 prototype aircraft, the model rotor hub contour follows the full scale hub geometry closely.

The model support basically consists of the DNW open jet common support housing structure, a vertical mast, angle of attack hinge point and vertical sting (figure 8).

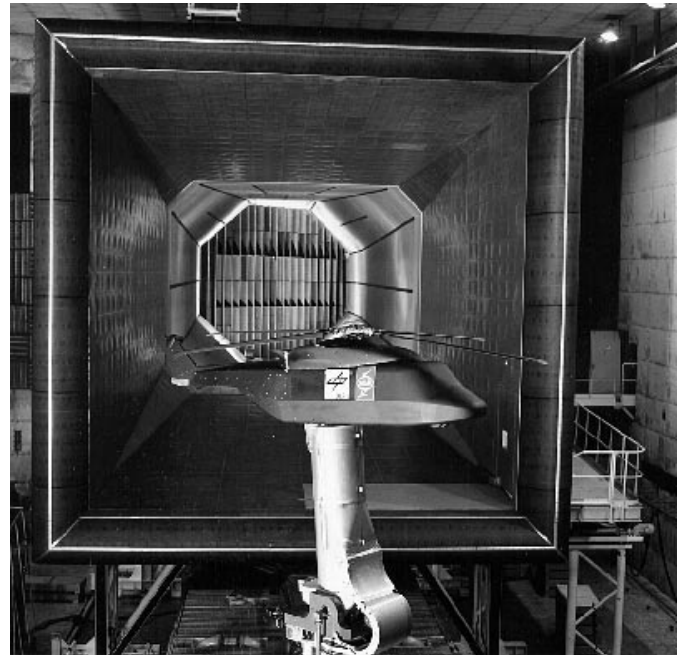


*Fig.8: Powered main rotor model in DNW (photo:DNW)*

The common support system allows testing in a wide range of sidewind conditions (270°) and a limited angle of attack range ( $\pm 10^\circ$ ).

The hub utilizes single spherical elastomeric bearings to allow the blade to pitch, lead-lag and flap. The model bearings (Lord design) are composed of an inner and outer structural member and a spherical shaped elastomer/shim package made up of alternating layers of metal shims and layers of elastomeric materials.

The spring rates of the bearing, which are scaled down, are based primarily on the stiffness and deflection of the elastomeric layers.

The elastomeric material provides inherent damping, due to hysteresis and provides a service life with minimal, visual, on-condition inspection and replacement criteria. A set of elastomeric inter-blade lead-lag dampers, located between each 2 sleeves, has been worked into the hub design. Static and dynamic damping characteristics were matched to control the rotor system ground resonance.

The sleeve attaches the rotor blade to the rotor hub. It also provides attachments for the pitch lever and flapping stops. Flapping stops limit the blade angles. The rotor torque is transmitted to the rotor drive system MWM via the rotor mast, which is hollow to allow for internal routing of the instrumentation cables.

The rotor blades are geometrically and dynamically scaled

copies of the full scale blades. The model blade D-spar graphite epoxy layer distribution and orientation has been defined such that the full scale blade properties (mass and stiffness distribution) are matched closely. The blades are constructed of a foam D-spar core (torsion box), wrapped with uni-directional graphite epoxy prepreg material and a foam trailing edge core covered with a skin.

OA series airfoils are applied, with linear transition between the various airfoil sections. The blade is equipped with a cavity at the blade tip for balancing, tungsten leading edge counter weights and a brass trailing edge trim tab (at 0.8R).

Instrumentation wiring is plugged onto a printed circuit board (PCB), which is mounted inside the rotor beanie. This dedicated printed circuit board is the front-end of the DLR data acquisition system.

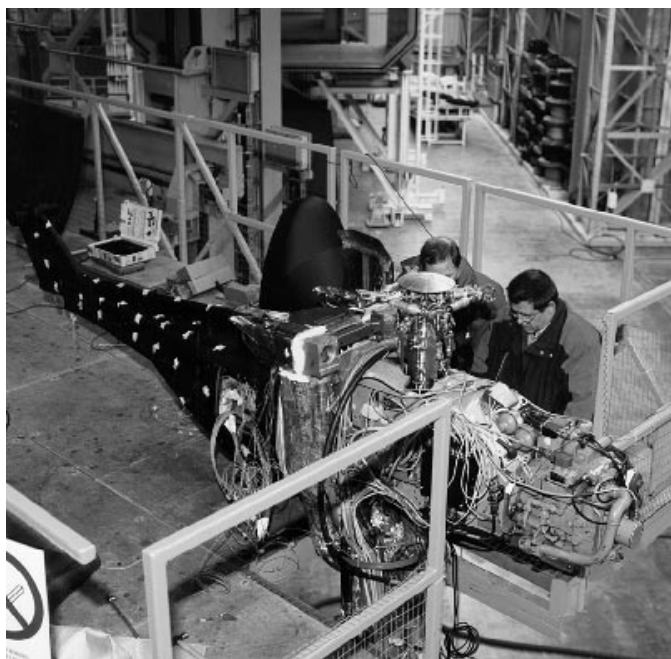


*Fig.9: Engine installation hardware integration (photo: NLR)*

Engine installation model hardware has been integrated in the fuselage hull (figure 9).

It consists of geometrically scaled down engine air intake and exhaust modules (external and internal geometry) and a capability to simulate representative engine intake and hot exhaust (upto 600 C) gas flow conditions.

The vacuum duct connects the intakes to a vacuum pump, which is located in the DNW test hall. Pressurized air is supplied by the DNW air supply system (ADS),

transferred through flexible hoses to the air heating system (located above the alpha knee). The central component of the air heating system is the burner can, in which propane gas is burned to heat the pressurized air to 600 C. The fuel controller is located inside the common support housing.

The engine cowlings are made of high temperature resistant glass reinforced epoxy. The air intake sub system consists of a detachable dynamic scoop, intake caisson, bellmouth and engine duct. The bellmouth is covered with an intake screen.

Behind the model compressor entry, the cross section area has been adapted to obtain the scaled mass flow capability.

The exhaust subsystem consists of a plenum settling chamber, perforated plate, which reduces the exhaust pressure from 6.5 to 1.0 bar, and a stainless steel nozzle.

All supply pipes, including MWM hydraulic lines and measuring cables are routed along the vertical strut and covered with a cylindrical fairing between fuselage model and alpha-knee.

#### Instrumentation

Instrumentation on the rotor blades consists of flap, chord and torsion strain gage bridges located at 5 different stations along two blades. Strain gage instrumentation wires run along the upper face of the D-spar core. This provides clean blade aerodynamics and a long life factor for the gages. Two remaining blades are equipped with "safety-of-flight" strain gage bridges in the blade root area.

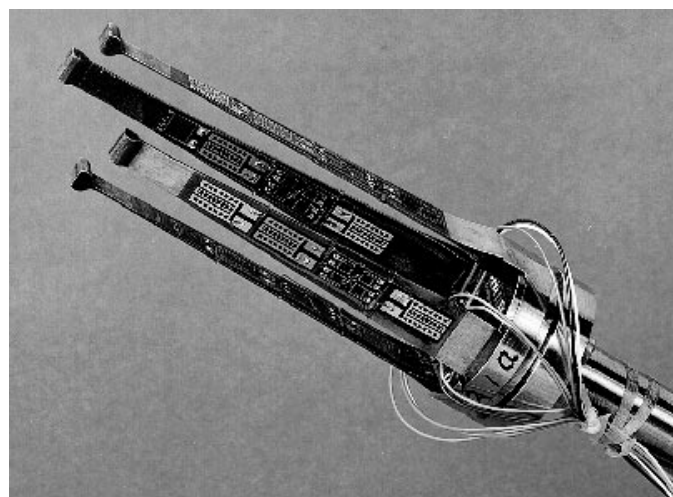


*Fig.10: Blade angle flexure system (photo: NLR)*

A unique flexure system has been developed, that fits in the hollow blade sleeve, to measure the blade angles (pitch, flap and lead-lag). The electronic components used to measure blade pitch is a resolver and strain gages to measure blade flapping and lead-lag. Two sets of instrumentation are located at opposite blades.

The blade angle measurement system is not sensitive to any translation of the sleeve, which during operation is introduced due to the elasticity of the elastomeric bearing. Achieved average accuracy of the angle measurement system is  $\pm 0.10$  (lead-lag) and  $\pm 0.15$  (flapping). The pitch angle measurement is performed by a resolver.

Two pitch links are instrumented with piezo electric transducers. Elastomeric bearings and dampers are equipped with thermo sensors to monitor component heating during rotor operation. To monitor the rotor mast bending, two strain gage bending bridges are installed on the rotor mast.

The MWM system includes a rotor balance (strain gauge load cells), to measure the rotor loads, torque meter and rotor rpm measurement. Global fuselage loads are determined by a 6 component Emmen balance. During engine installation testing, the Emmen balance was not used, but replaced by a dummy system. The horizontal tail vertical force is measured by a dedicated strain gage balance.

The fuselage was equipped with 76 thermo couples to measure the circulating air temperature.

The engine installation related instrumentation comprises of thermo sensors on the bellmouth screen, in the exhaust nozzle plane and on the cowling and fuselage skin. Both compressor entries are equipped with 6 rakes, each containing 2 total pressure tubes and a five hole probe to measure air intake gyration and flow distortion. The model furthermore is equipped with instrumentation for monitoring purposes.

### **Exhaust reingestion model (scale 1:10)**

#### Test objectives

The primary test objectives of the scale 1:10 recirculation model are:

- estimation of the probability of exhaust gas re-ingestion by the air intakes (particularly in the event of tail winds or rearwards flight);
- evaluation of the fuselage heating by these hot gases in flight conditions near hover (i.e. with sideways or rearwards wind);
- measurement of the infra-red signature.

Testing of various component configurations allows

design optimisation in an early stage of the development.

#### Model description

A scale 1:10 model was used to evaluate the exhaust gas reingestion in the air intakes and airframe heating in ECF low speed tunnel (figure 11).

The flight envelope explored in the wind tunnel corresponds to the wind envelope specified in the helicopter development contract.

The model was installed in the centre of the test section of the ECF wind tunnel in Marignane (Eiffel wind-tunnel). The fuselage is fitted to the lower mast via the support plate. The 6-axis balance is not used, since no force or moment are to be measured during the testing campaign.



*Fig.11: Engine recirculation model in ECF wind tunnel (photo: Eurocopter)*

A platform is located below the fuselage in order to place the model inside ground effect. The distance between the model and the platform can be adjusted in order to simulate a height of around 10 ft. Model features include air suction through the engine intakes and exhaust gas simulation with the proper mass flow and temperature characteristics. Rotor downwash has been generated by a generic, 2 bladed rotor system, mounted at the tunnel ceiling.

The model basic assembly, manufactured at scale 1:10 representing the NH90 airframe, consists of a fuselage, landing gear fairings, the fin and tail-plane, manufactured from glass-reinforced plastic. Engine cowlings, in which openings are incorporated to simulate the air intakes, are also manufactured from glass-reinforced plastic.

Engine exhaust jet-pipes, attached to the rear fairing, are manufactured from sheet steel. Different jet-pipe geometries may be adapted to the rear fairing, the jet-pipes themselves are directionally adjustable.

A generic twin-bladed rotor is fitted above the airframe, in order to simulate the mean induced airflow (the 1.5 [m] rotor diameter is close to the size of the NH90 main rotor at scale 1:10).

The air suction system is connected to the air intakes, this enables various engine inlet flows to be simulated, which at this scale are quite low. The suction is generated by a simple industrial vacuum cleaner. The hot gas exhaust system is connected to the jet-pipes. It enables the engine exhaust flow and the exhaust gas temperatures to be simulated.

Additionally, possible exhaust gas dilution can be represented by increasing the flow and decreasing the temperature. The exhaust gases are heated by 2 gas burners.

The exhaust modules are detachable, allowing the evaluation of various configurations.

#### Instrumentation

The fuselage is fitted with approximately 75 thermocouples distributed over the engine cowlings and the rear part of the fuselage (dog kennel, tailboom, fin and tail-plane). The distribution of these sensors was optimised by a simplified preliminary calculation of the exhaust gas trajectories.

In order to avoid the effects of heat conduction in the model skin, which is not thermodynamically representative of the actual aircraft, the thermocouples are positioned a few millimetres away from the surface of the model, in order to measure the temperature of the surrounding airflow. The airframe temperature is then deduced from this measurement by calculation.

Additionally, the air inlet ducts are equipped with six thermocouples at each side. It is therefore possible to measure not only the average temperature rise during flight in the event of exhaust gas re-ingestion, but also to evaluate the temperature distortion. These two parameters (average and distortion) affect the installation losses and the engine operation.

Finally, each jet-pipe (figure 12) is fitted with a thermocouple in order to provide real-time measurement of the exhaust gas temperature.

In fact the test procedure involves measuring the temperatures dynamically during the exhaust gas temperature rise, data acquisition occurs as soon as the latter reaches the required temperature.

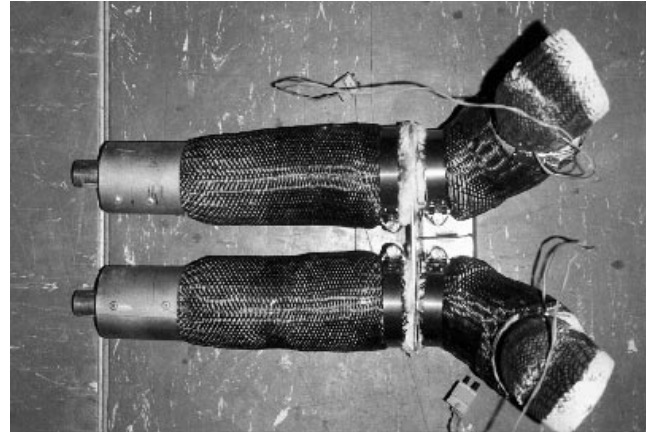


*Fig.12: Exhaust jet-pipes (photo: Eurocopter)*

The cold (suction) and hot (exhaust) airflows are measured using venturi systems (satisfying the requirements of standard NF X10.104).

#### **Air intake model (scale 1:3)**

##### Test objectives

The primary test objectives of the air intake wind tunnel model tests are:

- preliminary check of the engine inflow characteristics (pressure loss and distortion, flow gyration);
- estimation of the engine installation losses.

##### Model description

Detailed engine air intake flow characteristics were obtained using a 1:3 scale model in ECF low speed tunnel. Hover to high speed flight conditions were simulated during the wind tunnel trials. The model was built in such a way that modifications of air intake geometry were easily feasible. In consequence, optimization of the intake versus performance and inflow quality criteria was performed.

The model is mounted on top of the all purpose ECF wind tunnel sting. Because of the heavy weight of the model, additional supports are attached to tunnel hard points by mean of rods connected to the model and tunnel by rod eyes. In consequence, the 6 components external balance can give an estimation of the drag of the model (figure 13).

The model represents the forward part of the fuselage and the cowlings from nose radome to dog kennel. The skin is manufactured from glass-reinforced plastic. It is mounted on a rigid steel frame on which is also the hub system and the test apparatus are installed.

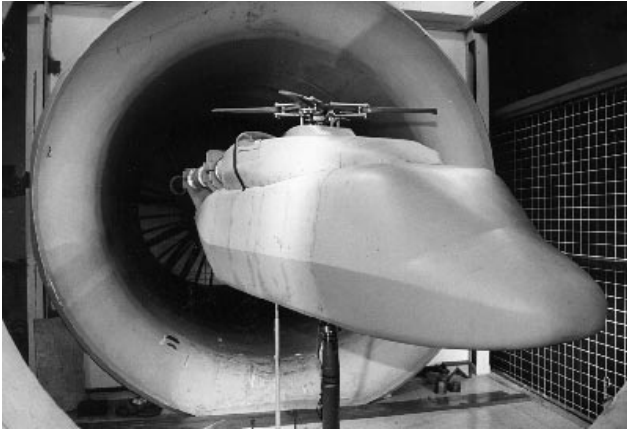


Fig.13: Air intake model in ECF wind tunnel (photo: Eurocopter)

The air intake geometry is accurately scaled down from the NH90 definition from the openings in the cowlings to the engine compressor entry (on the NH90, the bellmouth is considered as an helicopter part).

The NH90 air intake opening is on top of the cowlings and is protected by an outside grid. Inside the cowlings, the intake consists of a box like settling chamber, also called "caisson".

A bellmouth on which a secondary protective grid is fitted leads to engine compressor entry (figure 14).

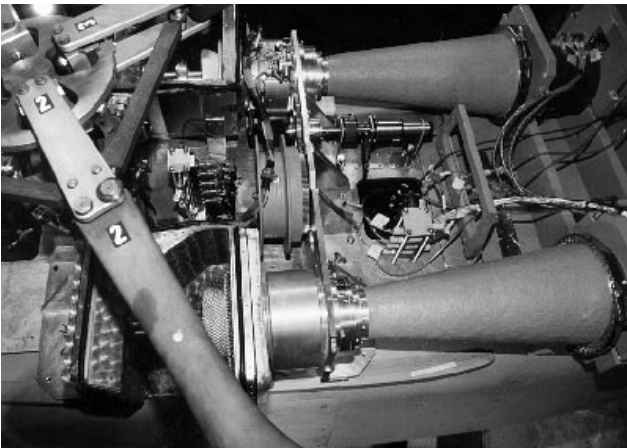


Fig.14: Air intake details (photo: Eurocopter)

An existing generic rotor hub with blade stubs is also present. The installation of a hub scaled from NH90 definition was not considered as mandatory. This hub is rotating at a speed close to the one of NH90 main rotor.

For each of the left and right air intakes, ventilators generate the scaled engine mass flow. For some configurations, because a high mass flow was desired while significant obstruction was present, it was necessary to install the two ventilators one behind the other (on right side).

#### Instrumentation

Only the right intake was instrumented, the other intake is connected to the ventilator to insure the proper symmetry of the airflow around the model.

The reference pressure was the atmospheric static pressure during the test sequence. It is measured by an altimeter, the reference temperature is the tunnel temperature.

In the intake, the static pressure is measured and an additional reference temperature is measured with a thermocouple.

The velocity field in the engine compressor entry plane (also called AIP, acronym for Aerodynamic Interface Plane) is measured with a five hole probe. The velocity field consists of pressure and direction of the local airflow at any location in the AIP. The probe is mounted on a sting, which is movable along a radius, the position is controlled by a step-by-step motor. This sub-assembly is fixed onto a rotating section which allowed an accurate azimuth positioning. In consequence, any radius/azimuth combination can be set and the whole compressor entry plane can be explored.

The probe is calibrated prior to each test campaign, the calibration accuracy is 1% for the pressure measurements and 0.5 for the gyration angle measurements (for the latter, the data remains valid up to 30 ).

The flow angles are calculated from the difference of pressures measured on two opposite location on the probe: 4 sensors give the differential pressures between top and bottom locations, left and right locations, right location and central (total) pressure value, total and static pressures. The tangential airspeed (gyration) is given by left minus right pressure measurements (through a calibration curve) and the radial airspeed by top minus bottom pressure measurements.

The mass flows generated by the ventilators were monitored through venturi's. The mass flows were corrected for the temperature increase in the ventilators (thanks to a dedicated temperature measurement).

## Application of test results

The following sections discuss how wind tunnel test results obtained with the models described, have been applied in the development of the NH90 helicopter.

### External geometry optimization

During the project definition phases the fall-out from the wind tunnel testing was essentially the establishment of the initial characteristics from trade-off studies and an assessment of the helicopter behaviour as compared to the targets (e.g. drag, stability requirements).

The evolution of the NH90 shape from the initial definition to the actual prototype is well described by the different fuselage models (scale 1:10), applied since the beginning of the project. The models have been extensively used throughout the program phases from the initial feasibility study to the final design and development.

The models of the preliminary phases are witness of the changes occurred in the helicopter shape (figure 15) during the definition of the project, most of them dictated by the progressive growth of the design and changes suggested as a result of the wind tunnel activities.

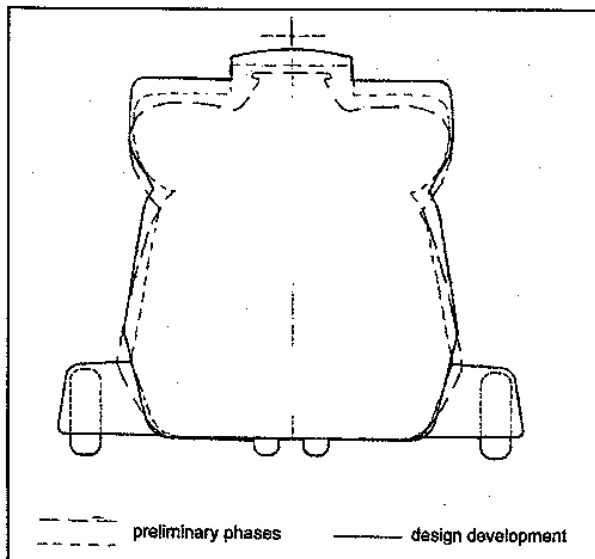


Fig. 15: Fuselage model cross section evolution

The upper deck evolved from a configuration with dynamic air intakes (largely separated engines) to a semipod shape with static air intakes. The sharp nose was progressively increased in volume and rounded, the tail plane finally positioned asymmetrically rearward. The

sponsons were enlarged to host the main landing gear, the additional requirement for a rear ramp was introduced in the aft fuselage.

At the beginning of the Design & Development phase, the geometry of the NH90 showed a general increment of the volume with increased frontal area of the upper deck and fuselage width, these features having a negative impact on drag and stability. An optimization of the aerodynamics of the fuselage was deemed necessary.

A specified task of optimisation of the external geometry was undertaken, supported by an extensive wind tunnel activity. Two main purposes were addressed: drag reduction and improvement of the longitudinal and lateral/directional stability characteristics.

Over a period of two years, from the start to the design freeze, five wind tunnel campaigns, performed on the fuselage model (1:10), allowed to evaluate several modifications in all the areas (cowlings, sponsons, tail surfaces, rear fuselage etc.) and to achieve a global aerodynamic improvement.

A significant reduction of the overall drag was obtained as a result of the wind tunnel test by:

- reducing the engine lateral separation and width in the exhaust area;
- rounding the planform shape of the sponsons, which also showed a positive effect on the lateral stability;
- changing the vertical fin airfoil and design of an enlarged profile-shaped fairing of the tail rotor gear box, which also was beneficial for the directional stability;
- optimizing the angle for the fuselage rear ramp;
- improving the design of the pylon/hub area, aimed at lowering the effect of the aerodynamic interferences;
- carefully paying attention to the aerodynamics of protuberances like fairings on the external equipments (e.g. nose FLIR, rescue hoist) and external devices (e.g. folding actuators on tail boom);
- filling up gaps of some cavities like landing gear bay and tail boom folding.

Specific tunnel tests were also dedicated to the sizing of the tail surfaces, in particular addressing type and location of the stabilizer, allowing for an improvement of stability characteristics and achievement of a good compromise between low speed and high speed longitudinal requirements (which in the meantime is confirmed by flight testing).

### Flight performance prediction

Helicopter flight performance capabilities are largely influenced by the drag value of the complete aircraft. To allow for an accurate performance prediction, the drag measured with a wind tunnel model has to be corrected. Unknowns are factors influencing the representativity of the experimental data gathered (e.g. due to Reynolds effects and engine intake pressure loss) or contributions of external components not yet selected or defined.

In the course of the project, the fuselage model representativity was enhanced and model components were detailed. The external contouring of the model converged to the definition of the present design, applied on PT1. This resulted in an increased fidelity of the global drag value, obtained from the various wind tunnel test campaigns and prior experience. At present the ratio of actual (measured) versus estimated drag contributions is appr. 75%. The drag breakdown of both TTH (left) and NFH (right) versions is shown in figure 16.

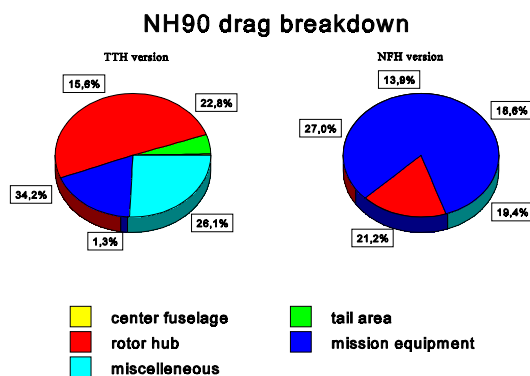


Fig.16: TTH and NFH drag breakdown

### Handling qualities

In an early stage of the D&D phase the ECF flight simulator SPHERE was used as a valuable tool to support handling quality related development work. Initial activities focused on verification of handling quality requirements, established by a joined Government-Industrial working group, who tailored the ADS 33 handling quality requirements to the specific NH90 situation. SPHERE also served as a development tool for the definition of the flight control laws. To accurately represent the NH90 flying characteristics a sophisticated flight simulation model should be used which is fed by a comprehensive aerodynamic database of the helicopter.

One fuselage model test campaign was dedicated towards the establishment of a fuselage and empennage aerodynamic database (global aerodynamic loads) at a wide range of angle of attack and sideslip conditions. Curve fitting was applied to the wind tunnel test results, to obtain a high order parametric representation of the airframe aerodynamic characteristics for inclusion in the simulation code.

Powered model test results (both with the main and tail rotor models) were used to validate the main rotor wake-stabilizer and tail rotor wake-vertical fin interaction models. Measurement of the stabilizer vertical load on the powered main rotor model, allowed a detailed analysis of the stabilizer behaviour during emersion into the rotor wake at low speed transition. Correlation of predicted trimmed low speed pitch attitudes with PT1 flight test results was good (accuracy approximately 1 ).

Testing of the tail rotor model at large sidewind conditions provided an elaborate rotor-fin aerodynamic interference database. Interactional characteristics were isolated and implemented as a parametric representation in the simulation code.

After one year of prototype flight testing, the availability of a high fidelity flight simulation model has proven to be very fruitful for both handling quality studies dedicated to design optimisation and intensive piloted simulation.

### Fuselage pressure distribution

To investigate the aerodynamic flow around the helicopter, during the D&D, a computational activity has been conducted. Results from these calculations were used in the selection of the pitot tube location and for the dimensioning of some structures like doors, sponsons and rear ramp.

Experimental data from the wind tunnel experiments have been profitably applied, in general, to verify the consistency of the analytical results and, in some cases, to refine the computational methodology and obtain improved outputs.

The Agusta VSAERO model of the NH90 helicopter has been applied which provides:

- surface pressure distribution;
- on and off-body streamlines;
- external flow characteristics on assigned off-body planes.

VSAERO is a potential-theory panel-method code for subsonic flow. The body is represented by panels on which the sources and doublets strengths are determined (figure 17).

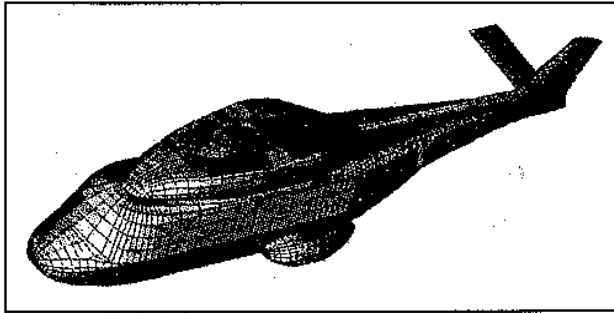


Fig.17: VSAERO panel distribution

Two-dimensional boundary layer, calculated along the surface streamlines can be coupled with the potential solution. Wake panels can be used to simulate separations; however the user is responsible for determining the starting location of the separated flow. For those cases where, due to the fuselage shape or the particular flight condition, a flow separation occurs, the code must also model the wake. This modelling is done by shedding a wake that convects downstream the vorticity released when the boundary layer separates. The quality of the final results from this approach depends on the ability to actually reproduce both the location where the wake leaves the fuselage and its trajectory.

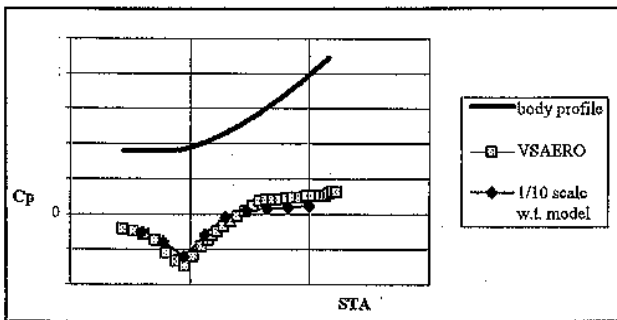


Fig.18: Correlation between calculation and experimental data at rear ramp (zero sideslip, angle of attack: -5 )

The fuselage pressure distribution was calculated e.a. in the rear ramp area, a region which generally induces separated flow. At small angles of attack and sideslip, the body is free from complex flow separation and the comparison between experimental and calculated pressure confirm that satisfactory results can be achieved from the computational code by using its own controls (figure 18).

At high attitudes, particularly in large sideslip conditions where complex interactions may occur between wake and body, an improvement of the analytical results is obtained by tuning the procedure on the basis of the wind tunnel measurements (figure 19).

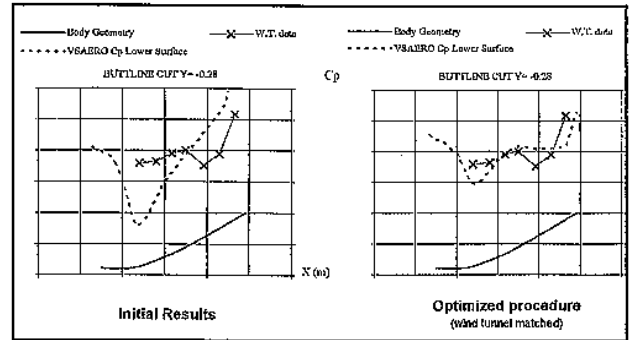


Fig.19: Results of data matching (at rear ramp location, sideslip: 45 , zero angle of attack)

Indications about the position of the stagnation points can be derived from experimental data, thus allowing for a better definition of the separation into the code and an optimisation of the computational model.

#### Aerodynamic loads on rear ramp

The NH90 TTH version will be equipped with a rear ramp, which is supposed to be operated (closed/opened) during flight. To support the establishment of the rear ramp design loads and to determine the impact of ramp operation during flight on helicopter performance and flying qualities, a dedicated wind tunnel test campaign with the fuselage model (1:10) was executed in the DNW-LST.

The starboard side of the ramp and hatch model parts are equipped with 45 static pressure holes in total (16 static pressure holes on the outer, 16 on the inner surface of the ramp, 12 on the outer, 1 on the inner surface of the hatch). Rear ramp test configurations are shown in figure 20.

The measurements were performed with the model upside-down (large sideslip angles:  $\pm 45^\circ$ ) and rolled on its side (large angles of attack:  $\pm 45^\circ$ ), in order to minimize the disturbing effect of the support sting on the flow around the ramp and hatch.



Test results showed an increase in drag especially for the configurations with the fully opened ramp and ramp removed. The static pitch stability of the model was not significantly influenced.

The side force increased at sideslip angles with a larger opening angle of the ramp because of the enlargement of the lateral area of the fuselage. Since this additional area is aft of the fuselage centre of gravity, the yaw stability (the yawing moment curve slope versus sideslip angle) increases.

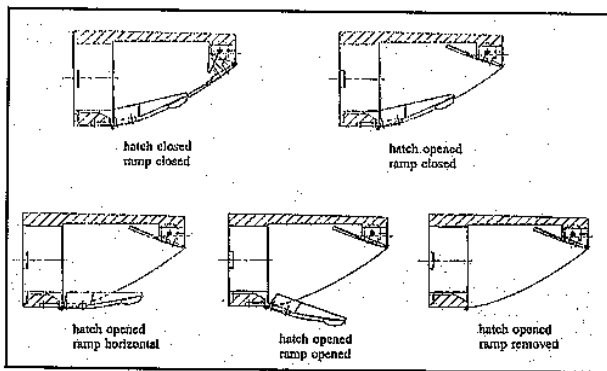


Fig.20: Model rear ramp test configurations

Ramp and hatch forces were obtained by integrating the pressures measured on the inner and outer surface of the ramp and hatch. The vertical forces, important for design load verification, are plotted in figure 21 for an angle of attack and sideslip range.

An important result for the design load specification of the ramp was that with the ramp in an open horizontal position, which is a required operational flight condition, no significant changes in the order of magnitude and direction of the vertical force compared to the closed ramp position was measured. Only if the ramp is opened completely the vertical upward force changes to a significant downward force for small sideslip angles. For both these ramp positions the vertical force on the corresponding open hatch is an order of magnitude smaller.

The wind tunnel investigation demonstrated the usefulness of relatively low cost wind tunnel simulation of a dedicated full scale helicopter component. Thus to reduce the development risk of failure of the ramp and hatch structure, joints and actuators of the full scale device under aerodynamic loading as well as possible deterioration of handling qualities of the actual aircraft due to the open ramp or hatch or both.

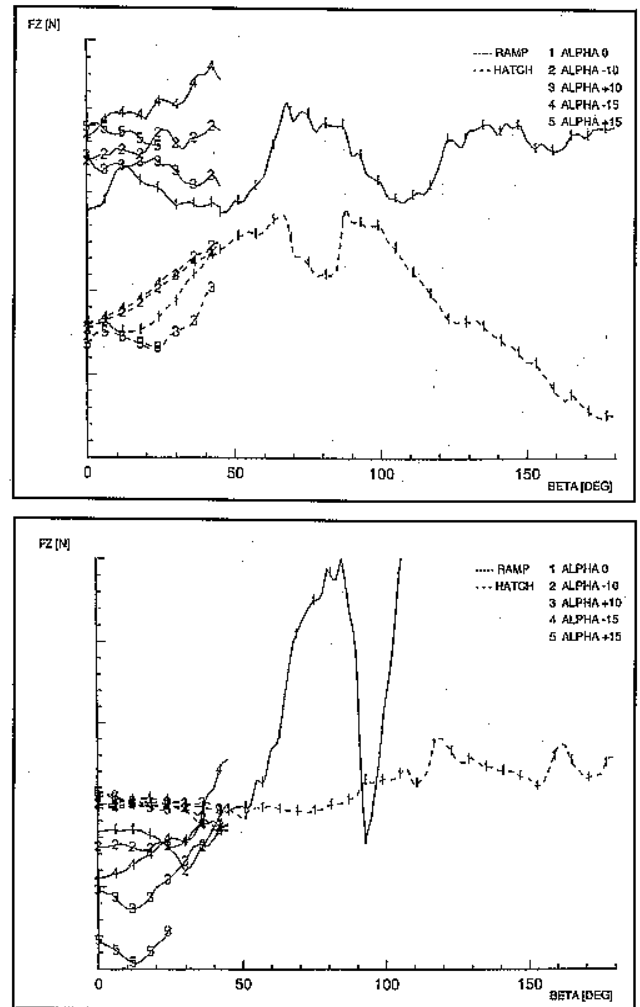


Fig.21: Rear ramp vertical force (open hatch, ramp horizontal (top) and closed (bottom))

### Engine exhaust gas recirculation and airframe heating

At sideward and rearward flight conditions hot exhaust gasses might re-ingest into the air intakes and locally heat the airframe structure.

During the course of the D&D a wind tunnel exploration of various exhaust configurations (with varying jet-pipe shape, length and orientation). This enables to select the optimal solution with respect to susceptibility to recirculation, but also provides back-up solutions compatible with other helicopter design constraints such as weight or installation losses.

Analysis of the wind tunnel test results enables the evaluation of the likelihood of exhaust gas recirculation in the air intake system.

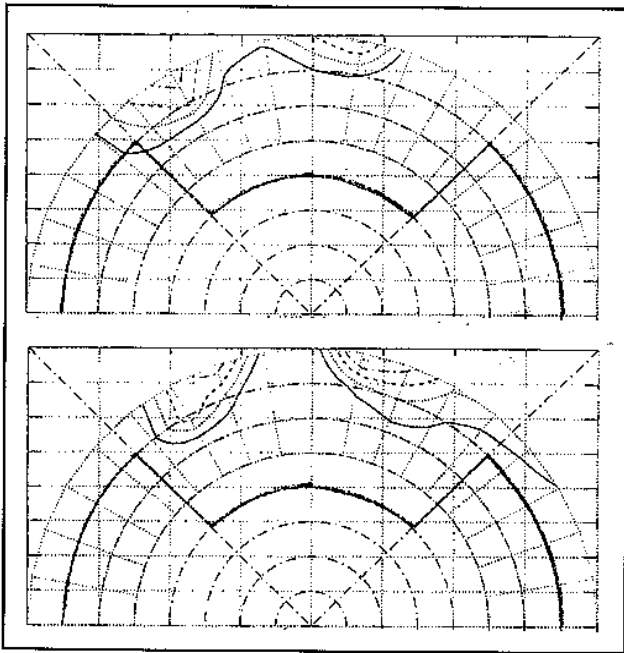


Fig.22: Air intake exhaust gas recirculation zones (LH - top- and RH -bottom- intake)

The graph (figure 22) shows the temperature increase measured in the model RH (right) and LH (left) air intakes at various tailwind azimuthal conditions. Each semi-circle represents a wind speed, the position on the semi-circle indicates the wind direction. For a given configuration of aircraft and jet-pipes, this graph shows the zones for which hot exhaust gas ingestion by the engine air intakes was measured.

This information is essential, since it enables the flight test crew of the prototype to be warned, for a given design, of the zones where hot gas recirculation is most likely to be encountered. In-flight exploration, and consequently development costs are therefore reduced.

Detailed analysis of the recirculation model fuselage thermo sensor data enables the evaluation of structural heating associated with the hot engine exhaust gas.

Sample results of such analyses, performed for a wide range of wind tunnel conditions (speed and direction) and helicopter and jet-pipe configurations, are illustrated in the graph below (figure 23). For tail wind conditions, the structural heating is represented in the form of a map (top) and temperature contour plot (bottom).

As for gas recirculation, it is possible to identify the parts of the helicopter flight envelope which are likely to be subjected to structural heating. This kind of testing also provide the maximum temperature encountered on the

helicopter and the precise location of the heated zone. The temperature measurement installation for the prototype flight testing can therefore be optimised.

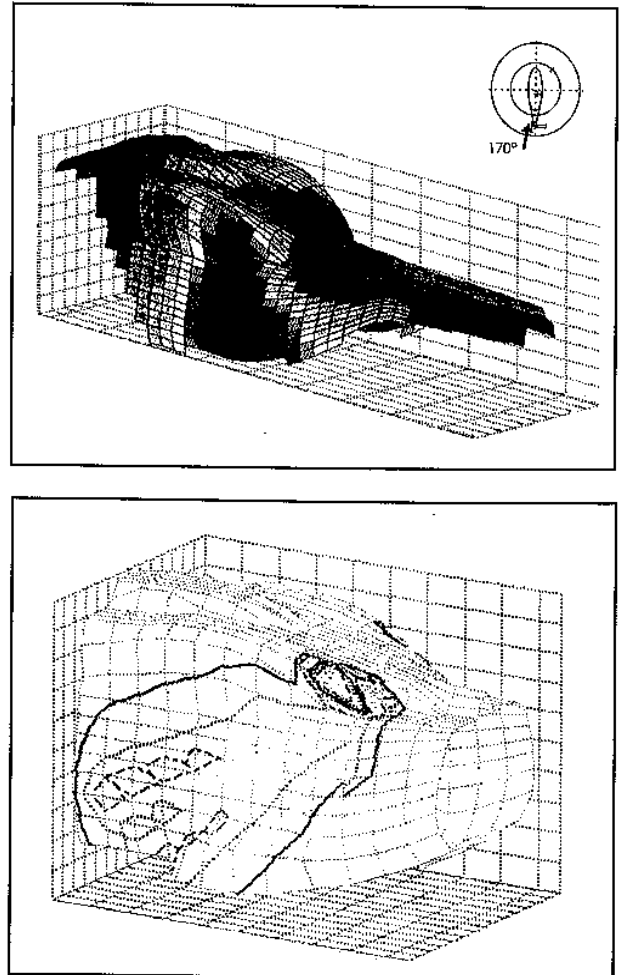


Fig.23: Airframe structural heating

Analysis of the wind tunnel test results enables the selection of the optimal solution of those configurations tested in the wind tunnel, appropriate material choice or possible application of local heat-shields.

Wind tunnel test results obtained, enable quickly design optimization, in terms of size and of effectiveness, for the prototype configuration.

#### **Air intake performance and flow quality**

Detailed engine air intake flow characteristics were obtained using a dedicated intake model. The aim of such a test is to verify the air intake operation with respect to engine criteria and if necessary to improve the definition. The parameters of interest for this study are the air intake pressure and swirl angle measurements (mean values and distortions).

The test matrix included helicopter speed, incidence angle, sideslip angle and engine air flow variations, allowing exploration of the complete helicopter flight envelope.

Figure 24 presents a sample swirl angle cartography measured in the aerodynamic interface plane of an air intake definition. Fluctuations shown on that figure indicate that the airflow is far from being homogeneous, but that typical swirl distortions around a mean value occur.

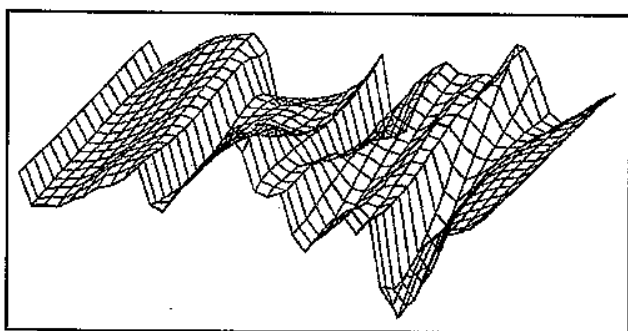


Fig.24: Sample air intake swirl angle cartography at 300 km/h (x-axis: azimuthal position, y-axis: radial position)

For some helicopter speed or engine power (air mass flow) conditions, air intake distortion can be important. Analysis of local air intake measurements (incl. pressure and the main distortion position) indicates the area of the air intake where improvements of the definition are necessary.

Detailed air intake test results can be further processed to some "global" parameters. This exploitation is necessary to reduce all the measurement results to a equivalent tests conditions and to correct the data to the full scale air intake performances. The results allow comparison with global engine criteria and evaluation of the engine installation losses.

Figure 25 shows the evolution of average pressure loss, average gyration, min/max gyration, average pressure distortion and min/max pressure distortion (from top to bottom) versus helicopter speed. The results can be compared to the engine criteria and if necessary lead to improvements of the definition.

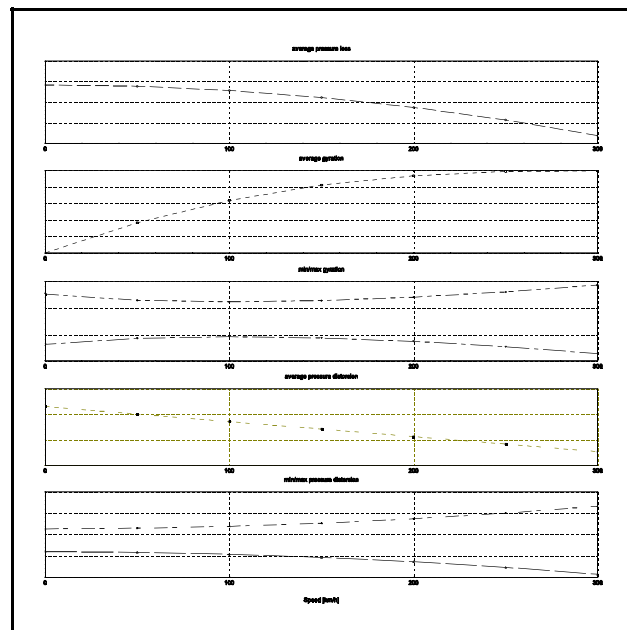


Fig.25: Trends of air intake installation losses versus speed

During wind tunnel testing the influence of some modifications of the intake definition can be measured and/or the influence of protrusions like protective grids can be studied. It is possible to anticipate in an early stage of the development to potential problems inherent to the air intake definition by correcting the definition.

Wind tunnel tests can provide an optimized air intake definition or, at least, a definition which will respect the engine installation criteria to a major extend.

### Concluding remarks

A series of wind tunnel test campaigns with both powered and unpowered models have been performed to support the NH90 design and development activities.

Helicopter aerodynamic characteristics could be determined in an early stage of the program, which contributed to a reduction of the development risks.

As a result of the wind tunnel experiments conducted, the helicopter external geometry was refined, tail surfaces were sized and positioned, air intake and exhaust configurations were optimized.

Experimental data furthermore were applied to validate aerodynamic computation methods (component design load sizing) and were fed into performance prediction and simulation codes.

Table 1: NH90 wind tunnel model synthesis

Characteristic\Model	Fuselage	Tail rotor	Main rotor	Recirculation	Intake
<b>MAIN ROTOR</b>					
scaling law (factor)	geometry (10)		geometry/Mach/Lock	mu	geometry
no. blades	4		4	2	4
radius	stubs only		2.10 [m]		stubs only
control angle(s)	coll & cyclic (preset)		coll & cyclic (remote)	collective (remote)	coll & cyclic (preset)
load balance	(see fuselage)		6 components	-	-
no. sensors	-		50		-
power @rpm	0.3 kW @ 1200 rpm		135 kW @ 1050 rpm	25 kW @ 1275 rpm	1 kW @ 340 rpm
<b>FUSELAGE</b>					
configuration	complete fuselage	tail cone, vertical fin and stabilizer	fuselage without sponson	complete fuselage	fuselage without sponsons/tail
scaling law (factor)	geometry (10)	geometry (3.881)	geometry (3.881)	geometry (10)	geometry (3)
no. stabilizer positions	4	1	3	1	-
load balance	6 component balance	6 component	6 component, 1 component stabilizer balance	-	-
no. pressure holes	125	-	22 (of which 6 unsteady)	-	-
no. temperature sensors	-	-	76	75	-
<b>TAIL ROTOR</b>					
scaling law (factor)	geometry (10)	geometry/Mach (3.881)	-	-	-
no. blades	4	4			
radius	blade stubs only	0.41 [m]			
control angle(s)	-	collective			
load balance	(see fuselage)	2 component			
no. sensors	-	6			
power @ rpm	-	13 kW @ 3000 rpm			
<b>ENGINE</b>					
scaling law (factor)			geometry (3.881)	geometry (10)	geometry (3)
air intake			air suction @ 0.40 kg/sec	air suction @ 0.020 kg/sec	air suction @ 0.65 kg/sec
exhaust			exhaust gas @ 600 C	exhaust gas @ 600 C	-
no. temperature sensors			18	2*6	-
no. pressure sensors			12 five-hole probes 24 total pres. probes	-	1 five-hole probe (movable), 2 total pres. probes
<b>MODEL SUPPORT</b>					
type	forward vertical belly sting	vertical sting	aft vertical/skewed belly sting	vertical sting	vertical sting
angle of attack range	± 20 ± 180 ; rolled model	-	± 10 /± 30	-	± 10
sideslip range	± 180 ± 20 ; rolled model	± 180	270 /± 30	360	± 10